

Conformational Studies by Dynamic NMR. 83.¹ Correlated Enantiomerization Pathways for the Stereolabile Propeller Antipodes of Dimesityl Substituted Ethanol and Ethers

Stefano Grilli,² Lodovico Lunazzi,* and Andrea Mazzanti*

Department of Organic Chemistry "A. Mangini", University of Bologna, Risorgimento, 4, Bologna 40136, Italy

lunazzi@ms.fci.unibo.it

Received April 23, 2001

Below $-100\text{ }^{\circ}\text{C}$, the NMR spectra of dimesityl derivatives of ethanol and of various ethers reveal how these molecules exist as M and P propeller-like stereolabile enantiomers, owing to the restricted rotation about the Ar–C bond. Single-crystal X-ray diffraction of one such derivative confirmed the existence of a two-blade propeller structure. Computer analysis of the NMR line shape allowed the barriers for the enantiomerization process to be determined. Theoretical modeling (Molecular Mechanics) of the interconversion circuit produced good agreement between the computed and experimental barrier for a correlated dynamic process where a disrotatory one-ring flip pathway reverses the helicity of the conformational enantiomers. Introduction of a configurationally stable chiral center allowed two distinct NMR spectra to be detected at appropriate low temperature for two stereolabile diastereoisomers.

Introduction

Compounds comprising three *ortho*-substituted phenyl groups bonded to a configurationally stable sp^3 atom (e.g., carbon or silicon) display dynamic processes involving the interconversion of stereolabile enantiomers, according to correlated pathways (cog-wheeling circuit) described by the so-called *n*-ring flip mechanisms.^{3–6} The corresponding barriers were reported⁷ to cover the range 9–22 kcal mol^{-1} .

We have recently shown that even when there are only two *ortho*-substituted phenyl groups bonded to a tetrahedral center, like a sulfur atom, an analogous dynamic process does take place. Thus, in the case of dimesityl sulfoxide and sulfone a cog-wheel effect, which allows the interconversion of the two M and P propeller-like antipodes (conformational enantiomers) through the one-ring flip mechanism, was detected.⁸ In these cases, however, the enantiomerization barriers are much lower,

having ΔG^{\ddagger} values equal to 4.5 and 5.0 kcal mol^{-1} , respectively, for dimesityl sulfoxide and dimesityl sulfone. On the basis of the latter results it seems conceivable to foretell that a similar effect would also occur when two mesityl groups are bonded to a sp^3 hybridized carbon atom, since stereolabile helical enantiomers are also expected to be available.^{9,10}

To obtain an experimental verification of this prediction and with the purpose of assessing the possible consequences of the related stereochemical properties, the dimesityl derivatives of ethanol (**1**), dimethyl ether (**2**), ethylmethyl ether (**3**), diethyl ether (**4**), and ethyl 2-methylbutyl ether (**5**) were investigated: $\text{Mes}_2\text{C}(\text{Me})\text{OH}$ (**1**); $\text{Mes}_2\text{CHOCH}_3$ (**2**); $\text{Mes}_2\text{C}(\text{Me})\text{OCH}_3$ (**3**); $\text{Mes}_2\text{C}(\text{Me})\text{OCH}_2\text{CH}_3$ (**4**); $\text{Mes}_2\text{C}(\text{Me})\text{OCH}_2\text{CH}(\text{Me})\text{Et}$ (**5**) (Mes = 2,4,6-trimethyl phenyl)

Results and Discussion

All these derivatives were found to display dynamic effects in their ^1H and ^{13}C NMR spectra: as an example of such temperature-dependent features, the ^{13}C spectra of **3** will be illustrated.

At ambient temperature down to $-30\text{ }^{\circ}\text{C}$ (Figure 1) three signals due, respectively, to the methyl bonded to the quaternary carbon (24.9 ppm), to the four methyls in the *ortho* position (23.0 ppm) and to the two methyls in the *para* position (19.0 ppm) are observed in the 19–26 ppm spectral region. Owing to the different relaxation times the intensity of these ^{13}C lines is not proportional

* To whom correspondence should be sent.

(1) Part 82. Casarini, D.; Lunazzi, L.; Mazzanti, A. *Angew. Chem., Int. Ed.* **2001**, *40*, 2536. Part 81. Grilli, S.; Lunazzi, L.; Mazzanti, A. *J. Org. Chem.* **2001**, *66*, 4444.

(2) In partial fulfillment of the requirements for the Ph.D. in Chemical Sciences, University of Bologna.

(3) (a) Sabacky, M. J.; Johnson, S. M.; Martin, J. C. Paul, I. C. *J. Am. Chem. Soc.* **1969**, *91*, 7542. (b) Rieker, A.; Kessler, K. *Tetrahedron Lett.* **1969**, 1227. (c) Kessler, K.; Moosmayer, A.; Rieker, A. *Tetrahedron* **1969**, *25*, 287.

(4) (a) Gust, D.; Mislow, K. *J. Am. Chem. Soc.* **1973**, *95*, 1535. (b) Finocchiaro, P.; Gust, D.; Mislow, K. *J. Am. Chem. Soc.* **1974**, *96*, 2165 and 2176. (c) Mislow, K. *Chemtracts Org. Chem.* **1989**, *2*, 151.

(5) (a) Boettcher, R. J.; Gust, D.; Mislow, K. *J. Am. Chem. Soc.* **1973**, *95*, 7157. (b) Hutchings, M. G.; Maryanoff, C. A.; Mislow, K. *J. Am. Chem. Soc.* **1973**, *95*, 7158. (c) Kates, M. R.; Andose, J. P.; Finocchiaro, P.; Gust, D.; Mislow, K. *J. Am. Chem. Soc.* **1975**, *97*, 1772. (d) Mislow, K. *Acc. Chem. Res.* **1976**, *9*, 26.

(6) Sedo, J.; Ventosa, N.; Molinos, Ma. A.; Pons, M.; Rovira, C.; Veciana, C. *J. Org. Chem.* **2001**, *66*, 1579.

(7) Oki, M. *Applications of Dynamic NMR Spectroscopy to Organic Chemistry*; VCH: Deerfield Beach, 1985; Chapter 5, p 226.

(8) Casarini, D.; Grilli, S.; Lunazzi, L.; Mazzanti, A. *J. Org. Chem.* **2001**, *66*, 2757.

(9) The two enantiomeric forms of the highly hindered derivatives $\text{Ar}_2\text{CH}-\text{COOH}$ (Ar = 2,4,2',4'-tetra-*tert*-butyl-6,6'-dimethylphenyl and cognates) could be separated at ambient temperature having racemization barriers in the range 21.5–22.9 kcal mol^{-1} (Akkerman, O. S.; Coops, J. *Rec. Trav. Chim.* **1967**, *86*, 755. See also: Akkerman, O. S. *Rec. Trav. Chim.* **1970**, *89*, 673.).

(10) Dynamic processes were detected in the $\text{ArAr}'\text{CHMe}$ and $\text{ArAr}'\text{CHOH}$ derivatives (where $\text{Ar} \neq \text{Ar}'$), see: Finocchiaro, P. *Gazz. Chim. Ital.* **1975**, *105*, 149.

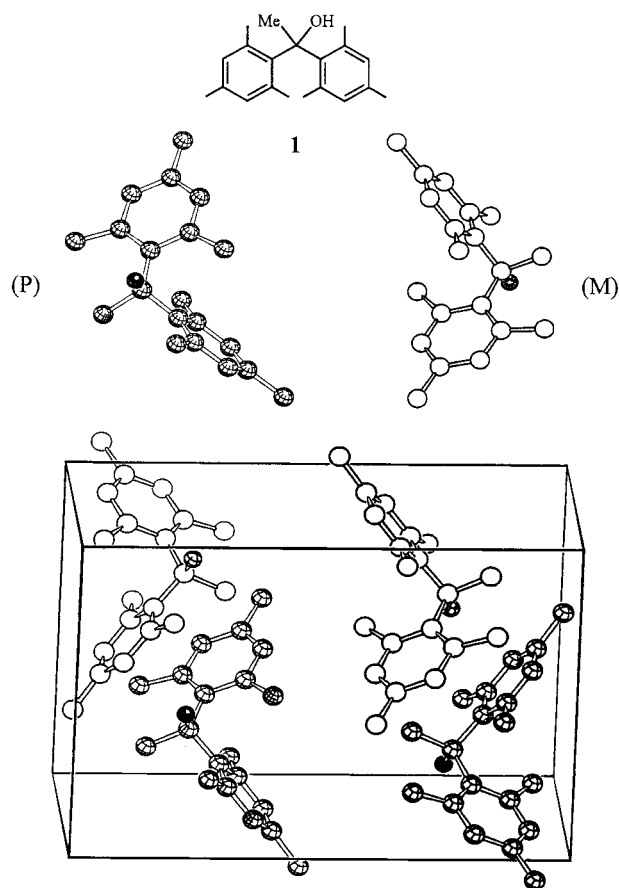


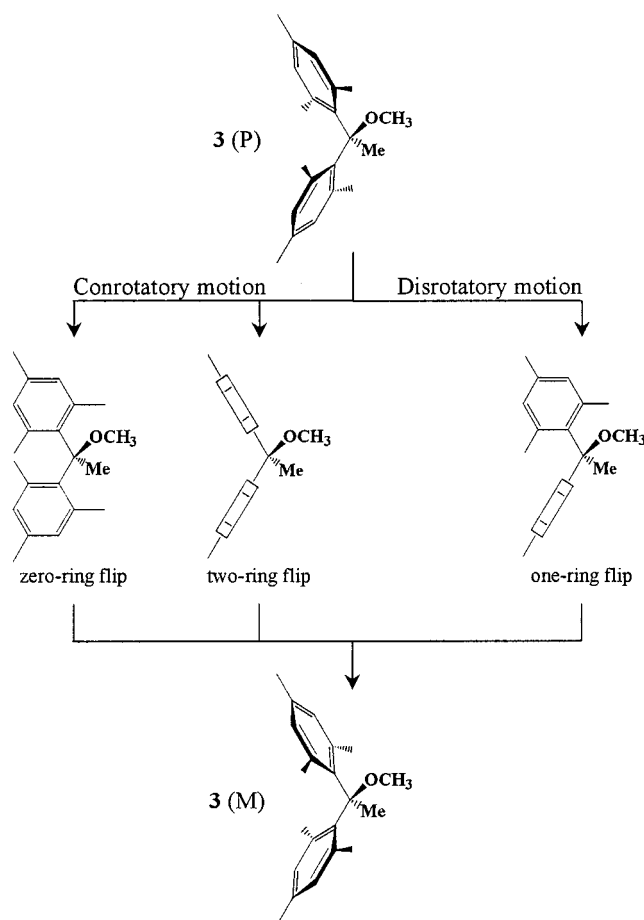
Figure 3. Computed structures (Molecular Mechanics¹¹) of the P and M enantiomers of **1** (top). Underneath is reported the experimental structure (X-ray diffraction) of the four molecules within the crystal cell. In both the computed and experimental structures the carbons of the enantiomer P are shaded dark whereas those of the enantiomer M are represented as colorless.

helical shape, the corresponding dihedral angles measured in the crystalline state (46° and 55°) being close to those computed for the isolated molecule. The crystal cell of **1** contains in fact four molecules, two of them having a helicity opposite to that of the other two (heterochiral crystals). In Figure 3 the M and P conformational enantiomers predicted by calculations are displayed together with the experimental structures of **1**.

As mentioned, the interconversion of these M and P stereolabile enantiomers is expected to occur through a correlated rotation process (cog-wheeling circuit) of the two mesityl groups. In principle three possible pathways are available: they can be classified according to the n -ring flip mechanisms reported in Scheme 1, where n can be 0, 1, or 2.^{12–14}

The zero-ring flip pathway is a conrotatory motion that not only leads to a very crowded transition state (coplanar mesityl rings) but, in addition, does not allow for the exchange of the *ortho* and *meta* edge positions, so that, being “NMR silent”,^{12,13b,14} cannot account for the observed dynamic process. The choice is thus restricted to

Scheme 1. Schematic Representation of the Ring Flip Circuit of **3**



the one- and two-ring flip mechanism and, to decide which one is expected to have the transition state with the lower energy, the dynamic process was modeled according to a Molecular Mechanics¹¹ approach.

In Scheme 2 is displayed the two-dimensional contour plot, derived from the three-dimensional energy surface computed as function of the two rotation angles between the mesityl rings and the C1–C(OMe)–C1' plane of **3**.¹⁵ The dotted line between the energy minima corresponding to the M and P enantiomers represents the two-ring flip mechanism, which is a conrotatory motion leading to a transition state where both the mesityl rings are orthogonal to the C1–C(OMe)–C1' plane (gear clashing). The computed barrier for this process ($18.2 \text{ kcal mol}^{-1}$) is much too high to be compatible with the experimental value. The full line is that for the one-ring flip mechanism, which is a disrotatory motion where the enantiomerization takes place via a transition state having one ring orthogonal to and the other coplanar with the mentioned plane (gear meshing). This process obviously entails a degenerate transition state where the two rings switch their relative position.¹⁶ The corresponding computed barrier ($7.6 \text{ kcal mol}^{-1}$) is much lower than the previous one and essentially coincides with that (7.45 kcal

(12) Nugiel, D. A.; Biali, S. E.; Rappoport, Z. *J. Am. Chem. Soc.* **1984**, *106*, 3357.

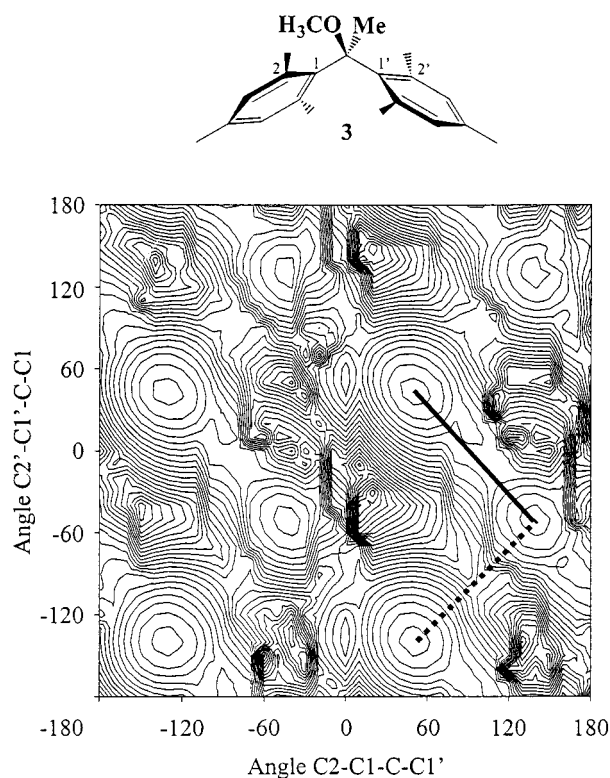
(13) (a) Rappoport, Z.; Biali, S. E. *Acc. Chem. Res.* **1988**, *21*, 442 (b) Rappoport, Z.; Biali, S. E. *Acc. Chem. Res.* **1997**, *30*, 307.

(14) (a) Grilli, S.; Lunazzi, L.; Mazzanti, A.; Casarini, D.; Femoni, C. *J. Org. Chem.* **2001**, *66*, 488. (b) Grilli, S.; Lunazzi, L.; Mazzanti, A.; Mazzanti, G. *J. Org. Chem.* **2001**, *66*, 748.

(15) The rotation barrier about the C–OMe bond was computed to be too low (2 kcal mol^{-1}) to be detectable by NMR spectroscopy. Thus the observed dynamic spectral features only depend on the restricted rotation involving the mesityl rings.

(16) Kaftory, M.; Nugiel, D. A.; Biali, S. E.; Rappoport, Z. *J. Am. Chem. Soc.* **1989**, *111*, 8181. Rappoport, Z.; Biali, S. E.; Kaftory, M. *J. Am. Chem. Soc.* **1990**, *112*, 7742.

Scheme 2. Two Dimensional Contour Plot of the Energy Surface of **3**, Computed as Function of the Dihedral Angles Made by the Mesityl Substituents with the C1–C(OMe)–C1' Plane^a



^a The full and the dotted line represent the one-ring and the two-ring flip pathway, respectively.

mol⁻¹) measured by the dynamic NMR experiment. As a consequence the latter mechanism is the most plausible pathway for accomplishing the M, P enantiomerization in derivative **3**.

The computations of the energy surfaces for derivatives **1** and **2** gave similar results: the corresponding data have been collected in Table 1.

These observations entail two stereochemical consequences that we were able to verify experimentally.

(i) If a prochiral probe,¹⁷ such as an ethyl group, is introduced in an appropriate position, the existence of the molecular asymmetry should be also revealed by the anisochronicity of the signals of the two methylene hydrogens. Thus in 1,1-dimesityl diethyl ether, (**4**) the quartet of the CH₂ group (coupled to the Me triplet with a vicinal $J = 7.1$ Hz) broadens on cooling and eventually splits into a pair of separate multiplets (displaying an additional J geminal coupling of -7.9 Hz) at -130 °C (Figure 4): the two geminal hydrogens become in fact diastereotopic when the interconversion of the M and P enantiomeric conformers is blocked. Since the source of the diastereotopicity for the hydrogens within the methylene moiety corresponds to the same restricted rotation process which makes the conformational antipodes sufficiently long living in the NMR time-scale, the barrier obtained by monitoring the methylene signals must be the same as that derived by monitoring the *ortho* methyl signals of the mesityl groups. Actually the two values (8.1

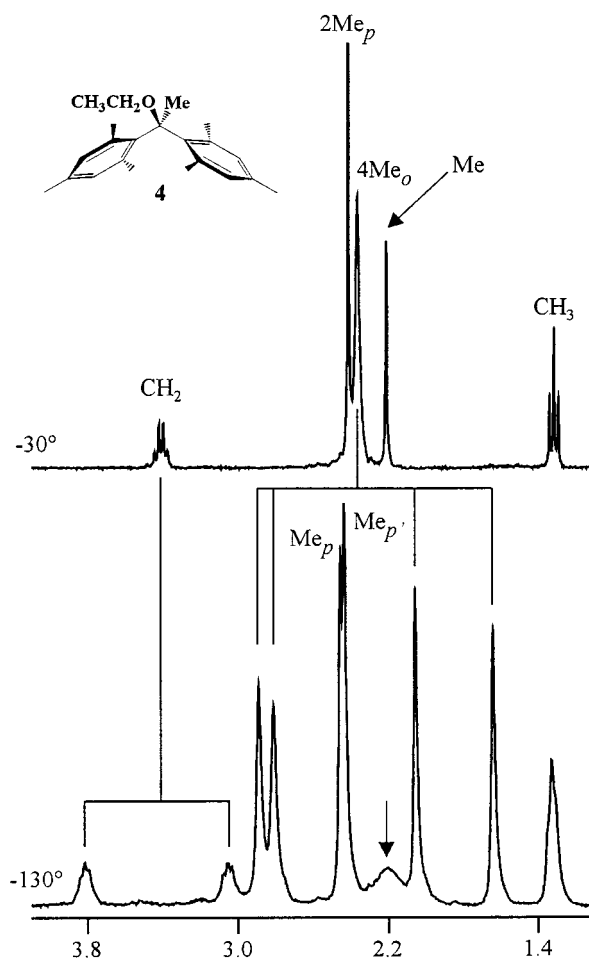


Figure 4. ¹H NMR spectrum (300 MHz in CHF₂Cl) of **4** at two different temperatures. Not only the para methyl signal splits into two and the ortho signal into four lines at -130 °C, but also the quartet signal of the hydrogens of the CH₂ group splits into two multiplets. (At this temperature the arrowed single line of the methyl group bonded to the quaternary carbon broadens considerably).

and 8.3 kcal mol⁻¹, respectively, as in Table 1) were found coincident within the experimental errors (± 0.15 kcal mol⁻¹).

(ii) If a configurationally stable chiral center is introduced in the molecule, it is expected that two stereolabile diastereoisomers become observable at a temperature where the rate for the propeller interconversion is rendered slow: this is because two sources of chirality would be simultaneously present. Derivative **5** fulfils these conditions since the aliphatic methine carbon is a configurationally stable chiral center. Actually the low temperature ¹³C spectrum of **5** displays a number of lines much greater than those expected for a single species. In particular it can be observed (Figure 5) that the single line of the mentioned methine carbon broadens on cooling and decoalesces, eventually yielding two lines (separated by 0.265 ppm at -114 °C) with a 53:47 intensity ratio. These lines are due to the pair of conformational diastereoisomers RM and RP (Scheme 3): each of them also comprises an enantiomeric form (respectively SP and SM). Molecular Mechanics calculations¹¹ suggest that the pair RM \equiv SP should be slightly more stable than the pair RP \equiv SM, the computed energy difference being 0.03 kcal mol⁻¹. Although such a difference corresponds exactly to the relative conformer population observed at

(17) Jennings, W. B. *Chem. Rev.* **1975**, 75, 307.

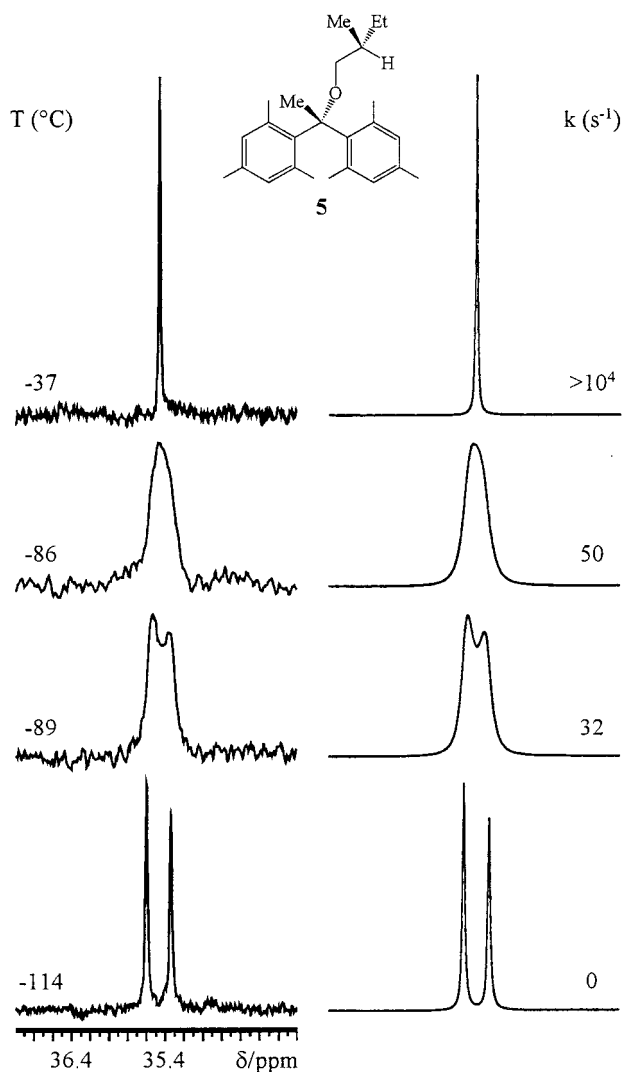


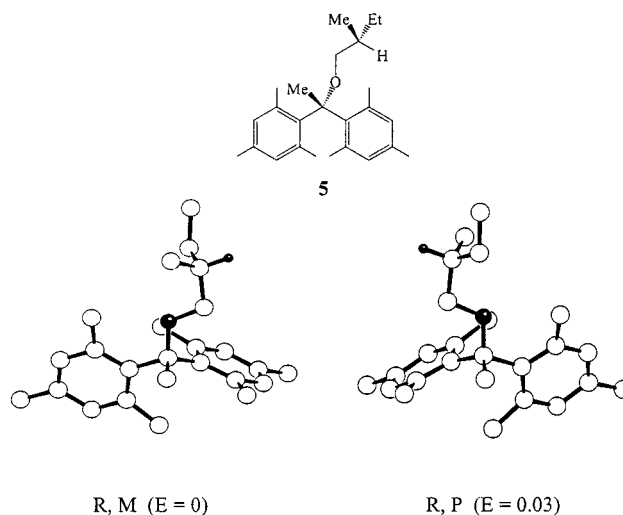
Figure 5. Left: experimental ^{13}C signal (100.6 MHz in $\text{CHF}_2\text{-Cl}$) of the aliphatic CH carbon of **5** as a function of temperature, eventually showing two lines (ratio 53:47) corresponding to the two diastereoisomers of Scheme 3. Right: line shape simulation obtained with the rate constants reported.

−114 °C, the smallness of this computed value does not allow one to exclude that the good agreement is the consequence of an accidental coincidence.

The line shape simulation of the two ^{13}C methine lines of **5** yields the rate constants, hence the free energy of activation, required to interconvert the two diastereoisomers (9.3 kcal mol $^{-1}$). The barrier must be the same as that obtained by monitoring, for instance, the lines of the *ortho* methyl signals, since the pathways for interconverting the diastereoisomers is the same ring-flip mechanism involving the mesityl groups. Within the experimental uncertainty, the latter value (9.5 kcal mol $^{-1}$) was found indeed equal to the previous one (Table 1).

The interconversion barriers measured in these compounds are significantly dependent upon the steric hindrance. Since derivative **5** bears an oxygen-bonded substituent (−CH $_2$ CHMeEt) quite bulkier than the methyl group of **3** or the ethyl group of **4**, the corresponding free energy of activation turns out to be appreciably higher (respectively by 2.0 and 1.2 kcal mol $^{-1}$). Likewise, substitution of the methine hydrogen atom of **2** with a methyl group in **3** makes the barrier of the latter 3.0 kcal

Scheme 3. Computed Structures (Molecular Mechanics¹¹) of the R, M (more stable) and R, P (less stable) Diastereoisomers of **5^a**



^a The relative values of the computed energies (*E*) are in kcal mol $^{-1}$.

mol $^{-1}$ higher. Also, replacement of the OH group of **1** with the OMe group in **3** increases the barrier by 1.6 kcal mol $^{-1}$ (Table 1).

Experimental Section

Materials. 1,1-Dimesitylethanol, (**1**) was prepared as reported in the literature.¹⁸ Products **2–5** were prepared according to the following procedure. To a suspension of KH (3 mmol in 5 mL of anhydrous THF), a solution of 1,1-Dimesitylethanol (1 mmol in 2 mL of anhydrous THF) was slowly added at 0 °C. After 10 min a solution of dibenzo-18-crown-6 (1 mmol in 5 mL of THF) was added and the mixture warmed to room temperature. After stirring for 30 min, the appropriate electrophile (MeI, EtI, 2-methyl-1-butyl-tosylate,¹⁹ 5 mmol in 2 mL of anhydrous THF) was added, and the mixture stirred for 3–6 h until the starting product disappeared (TLC). After quenching with water, the organic layers were extracted (Et $_2$ O), dried (Na $_2$ SO $_4$), and evaporated at reduced pressure. The crude products were purified on preparative TLC (eluent: pentane) to give the products in 20–50% yields. Note: the products are extremely sensitive to acidity to give 1,1-dimesityl-ethylene.

Dimesitylmethyl Methyl Ether (2). ^1H NMR (200 MHz, CDCl $_3$, 22 °C, TMS): δ = 2.08 (s, 12H, *o*-CH $_3$), 2.19 (s, 6H, *p*-CH $_3$), 3.29 (3H, s, OCH $_3$), 5.60 (1H, s CH), 6.72 (s, 4H, CH). ^{13}C NMR (50.3 MHz, CDCl $_3$, 22 °C, TMS): δ = 19.8 (*p*-CH $_3$), 19.9 (*o*-CH $_3$), 56.0 (OCH $_3$), 81.0 (CHO), 129.8 (CH), 135.9 (q), 136.9 (q), 143.8 (q). Anal. Calcd. For C $_{20}$ H $_{26}$ O: C, 85.06; H, 9.28. Found: C, 85.01; H, 9.26.

1,1-Dimesitylethyl Methyl Ether (3). ^1H NMR (200 MHz, C $_6$ D $_6$, 22 °C, TMS) δ = 1.87 (s, 3H, CH $_3$), 2.10 (s, 6H, *p*-CH $_3$), 2.22 (s, 12H, *o*-CH $_3$), 2.86 (3H, s, OCH $_3$), 6.69 (s, 4H, CH). ^{13}C NMR (50.3 MHz, C $_6$ D $_6$, 22 °C, TMS): δ = 21.0 (CH $_3$), 24.7 (*o*-CH $_3$), 26.6 (*p*-CH $_3$), 48.8 (OCH $_3$), 87.4 (q), 132.7 (CH), 136.0 (q), 137.3 (q), 142.3 (q). Anal. Calcd. For C $_{21}$ H $_{28}$ O: C, 85.08; H, 9.52. Found: C, 85.05; H, 9.56.

1,1-Dimesitylethyl Ethyl Ether (4). ^1H NMR (300 MHz, C $_6$ D $_6$, 22 °C, TMS) δ = 1.01 (t, *J* = 6.9 Hz, 3H, CH $_3$), 1.91 (s, 3H, CH $_3$), 2.10 (s, 6H, *p*-CH $_3$), 2.24 (s, 12H, *o*-CH $_3$), 3.09 (q, *J* = 6.9 Hz, 2H, CH $_2$), 6.70 (s, 4H, CH). ^{13}C NMR (75.5 MHz, C $_6$ D $_6$, 22 °C, TMS): δ = 16.0 (CH $_3$), 20.5 (CH $_3$), 24.4 (*o*-CH $_3$), 26.8 (*p*-CH $_3$), 56.9 (CH $_2$), 86.5 (q), 132.2 (CH), 135.4 (q), 136.7

(18) Timberlake, J. W.; Pan, D.; Murray, J.; Jursic, B. S.; Chen, T. *J. Org. Chem.* **1995**, *60*, 5295.

(19) Nakamura, Y.; Mori, K. *Eur. J. Org. Chem.* **1999**, 2175

(q), 142.3 (q). Anal. Calcd. For $C_{22}H_{30}O$: C, 85.11; H, 9.74. Found: C, 85.08; H, 9.77.

1,1-Dimesitylethyl-2-methylbutyl Ether (5). 1H NMR (300 MHz, C_6D_6 , 22 °C, TMS) δ = 0.75 (t, J = 7.4 Hz, 3H, CH_3), 0.88 (d, J = 6.8 Hz, 3H, CH_3), 1.00–1.14 (m, 1H, CH), 1.29–1.56 (m, 2H, CH_2), 1.96 (s, 3H, CH_3), 2.10 (s, 6H, p - CH_3), 2.25 (s, 12H, o - CH_3), 3.02 (m, 2H, CH_2), 6.70 (s, 4H, CH). ^{13}C NMR (75.5 MHz, C_6D_6 , 22 °C, TMS): δ = 11.6 (CH_3), 17.6 (CH_3), 20.5 (CH_3), 24.5 (o - CH_3), 26.8 (CH_2), 26.9 (p - CH_3), 36.0 (CH), 67.2 (CH_2), 86.8 (q), 132.1 (CH), 135.4 (q), 136.7 (q), 142.3 (q). Anal. Calcd. For $C_{25}H_{36}O$: C, 85.17; H, 10.29. Found: C, 85.13; H, 10.32.

X-ray Diffraction. Crystal Data for 1,1-dimesityl-1-ethanol (**1**): $C_{20}H_{26}O$ (282.41), monoclinic, space group $P2_1/c$, Z = 4, a = 8.6804(5), b = 15.9597(9), c = 11.8673(6) Å, β = 95.858(2), V = 1635.47(16) Å³, D_c = 1.147 g cm⁻³, $F(000)$ = 616, μ_{Mo} = 0.068 cm⁻¹, T = 293 K. Data were collected using a graphite monochromated Mo K α X-radiation (λ = 0.71073 Å) in the range $2.15^\circ < \theta < 30.08^\circ$. Of 21 769 reflections measured, 4791 were found to be independent (R_{int} = 0.1053), 1743 of which were considered as observed [$I > 2\sigma(I)$] and were used in the refinement of 198 parameters leading to a final R_1 of 0.0405 and a R_{all} of 0.1469. The structure was solved by direct method and refined by full-matrix least squares on F^2 , using SHELXTL 97 program packages. In refinements were used weights according to the scheme $w = [\sigma^2(F_o^2) + (0.0589P)^2 + 0.0000P]^{-1}$ where $P = (F_o^2 + 2 F_c^2)/3$. The hydrogen atoms were located by geometrical calculations and refined using a "riding" method. wR_2 was equal to 0.1328. The goodness of fit parameters S was 0.767. Largest difference density between peak and hole was 0.157 and -0.152 eÅ⁻³. Crystallographic data (excluding structure factors and including selected torsion angles) have been deposited with the Cambridge Crystallographic Data Center, CCDC 164872.

NMR Measurements. The assignment of the ^{13}C signals was carried out by DEPT sequence. The samples for the low-temperature measurements were prepared by connecting to a vacuum line the NMR tubes containing the desired compounds dissolved in some C_6D_6 or CD_2Cl_2 for locking purpose

and condensing therein the gaseous solvents by means of liquid nitrogen. The tubes were subsequently sealed *in vacuo* and introduced into the precooled probe of the 300 MHz spectrometer operating at 75.45 MHz for ^{13}C or 400 MHz operating at 100.6 MHz for ^{13}C . The temperatures were calibrated by substituting the sample with a precision Cu/Ni thermocouple before the measurements. Total line shape simulations were achieved by using a PC version of the DNMR-6 program.²⁰ Since at the low temperatures required to observe the exchange process the intrinsic line width of the compounds was significantly temperature dependent, the corresponding dependence of the solvent signal was measured. The appropriate ratio with the line width of the compound was then taken into account. We also checked that errors as large as 50% on this value affected the activation energy by less than 0.05 kcal mol⁻¹ in the temperature range investigated.²¹

Calculations. In the Molecular Mechanics computations¹¹ the dihedral drivers were obtained using a 10° rotational step over the bonds connecting the quaternary carbon to the mesitylene rings. In the case of the two diastereoisomers of derivative **5**, a search of the preferred conformation was performed by making use of the GMMX computer package (Serena Software, Bloomington, IN). The best structures were minimized again with the PC Model and cross-checked over the four possible stereoisomers in order to reduce the chances of slightly different final energy.

Acknowledgment. Thanks are due to the CNR I.Co.C.E.A. Institute (Bologna) for access to the 400 MHz spectrometer. Financial support has been received from MURST (national project "Stereoselection in Organic Synthesis") and from the University of Bologna (Funds for selected research topics 1999-2001).

JO010420M

(20) QCPE program No. 633, Indiana University, Bloomington, IN.

(21) Grilli, S.; Lunazzi, L.; Mazzanti, A. *J. Org. Chem.* **2000**, *65*, 3653.